AFRL-VS-TR-2002-1613

Design and Testing of a Low-Power DISS Sounder

B. Reinisch **G. Sales**

University of Massachusetts/Lowell
Center for Atmospheric Research
600 Suffolk St
Lowell, MA 01854

29 Feb 2002

Scientific Report No. 4

AIR FORCE RESEARCH LABORATORY
Space Vehicles Directorate
29 Randolph Rd
AIR FORCE MATERIEL COMMAND
Hanscom AFB, MA 01731-3010

REPORT DOCUMENTATION PAGE

Form Approved
OMB No. 0704-0188

1. REPORT DATE *(DD-MM-YYYY)*	2. REPORT TYPE	3. DATES COVERED *(From - To)*
20 -02-2002	Scientific, Interim	24 Sep 1998-23 Sep 1999

4. TITLE AND SUBTITLE
Design and Testing of Low Power DISS Sounder

5a. CONTRACT NUMBER
F19628-96-C-0159

5b. GRANT NUMBER

5c. PROGRAM ELEMENT NUMBER
61102F

6. AUTHOR(S)
Bodo Reinisch
Gary Sales

5d. PROJECT NUMBER
1010

5e. TASK NUMBER
IC

5f. WORK UNIT NUMBER
AA

7. PERFORMING ORGANIZATION NAME(S) AND ADDRESS(ES)
University of Massachusetts/Lowell
Center for Atmospheric Research
600 Suffolk Street
Lowell, MA 01854

8. PERFORMING ORGANIZATION REPORT NUMBER

9. SPONSORING/MONITORING AGENCY NAME(S) AND ADDRESS(ES)
Air Force Research Laboratory/VSBXI
29 Randolph Road
Hanscom AFB, MA 01731-3010

10. SPONSOR/MONITOR'S ACRONYM(S)

11. SPONSOR/MONITOR'S REPORT NUMBER(S)
AFRL-VS-TR-2002-1613

12. DISTRIBUTION/AVAILABILITY STATEMENT
Approved for Public Release; Distribution Unlimited

13. SUPPLEMENTARY NOTES

14. ABSTRACT
The Univesity of Massachusetts Lowell Center for Atmospheric Research investigated the design of a low power Portable Digital Sounder (LP-DPS) that would meet Air Force requirements for replacement of the FMQ-12 Digital Ionospheric Sounder network. The new system contains all the electronics in a single chassis. Multi-Dimensional Processing makes weighted decisions verifying that received signals are sounder echoes before passing them on for post processing analysis. The raw or partially processes samples were moved out of the DSP so that the next measurement could proceed while the Main or Auxiliary computer executes the DSP algorithms in parallel with the sounder's DSP operations. This required high-speed transfer of large quantities of data, which was accomplished by streamlining the data transfer protocol between the DSP board and the main computer. The present analog receivers will be replaced with a digital receiver chip.

15. SUBJECT TERMS
Ionosphere Ionosonde Profiles

16. SECURITY CLASSIFICATION OF:			17. LIMITATION OF ABSTRACT	18. NUMBER OF PAGES	19a. NAME OF RESPONSIBLE PERSON
a. REPORT	b. ABSTRACT	c. THIS PAGE			Balkrishna S. Dandekar
Uncl	Uncl	Uncl	Unl		19b. TELEPHONE NUMBER *(Include area code)* 781 377-2761

CONTENTS

1.0 Low Power Portable Digital Sounder Introduction

As a part of this contract, the University of Massachusetts Lowell Center for Atmospheric Research (UMLCAR), over the last year, investigated the design of a low power Portable Digital Sounder (LP-DPS) that would meet the Air Force's requirements for the future replacement of the FMQ-12 DISS network. There has been a Low Power DISS system, designed and built by UMLCAR (Digisonde DPS-4) operating at Ramey AB, Puerto Rico since May 1999. This system was considered a pre-production prototype for the LP-DISS replacement of the entire Air Force DISS network. As such it must perform the same functions, to the same degree of excellence, as the existing DISS system. The new system must also demonstrate a longer MTBF, lower maintenance and logistics costs, internal self-test capability, and an overall ease of operation that could be expected with such a drastic decrease in size and power and modernization of the circuitry.

The new LP-DISS is just over 50 kg and housed in a tactical transport case, which can be supplied with EMC shielding. The transmitted power is just over 100 W (100 to 150 W over the frequency band) vs. 10 kW for the older DISS. The new system contains all signal generation, computing and processing electronics in a single chassis, including the ARTIST and the Internet interface to the outside world. This design cleans up the proliferation of add-on computers that was required to give the older DISS the online data processing capability and Internet access. The entire LP-DISS system operates from a single 24V DC power source, typically directly connected to a battery for its source of power. This makes it:

- easy to backup through power outages
- operate in the field on battery power and from imperfect power sources
- immune to spikes, transients and line sags on the AC power mains

The following sections discuss improvements to the LP-DSP, addressing important issues encountered in the field operation of the sounder.

1.1 Multi-dimensional Data Processing

In addition to operational issues that are discussed below, several new design features were also considered for the next generation ionospheric sounding system. Since the DPS sounders produce multi-dimensional data describing several parameters that are used to characterize the received signals as sounder echoes vs. noise and interference, a new technique has been

developed that exploits these possibilities. The multi-dimensional processing (MDP) technique uses much of the large quantity of data available to make weighted decisions verifying that received signals are sounder echoes before passing them on for post processing analysis, such as ionogram scaling or plasma velocity calculation, etc. The fundamental signal characteristics considered are frequency, height/range, amplitude, phase, Doppler shift, wave polarization mode, and direction of arrival.

Two possible approaches were considered; first to implement the MDP algorithm on the sounder digital signal processor (DSP) board where the raw samples from the receiver output signals are collected. This approach eliminates the need to buffer up and move large volumes of raw data samples for processing by the Main Computer, or by an Auxiliary Computer, or for storage on disk/tape media. The second approach considered was to move all the raw or partially processed receiver samples out of the DSP such that the next measurement could proceed while the Main or Auxiliary computer executes the MDP algorithm in parallel with the sounder's DSP operations. Storing the raw samples also makes it possible to run the conventional processing algorithm or variations of new algorithms on exactly the same data sample so that a valid comparison of the various approaches can be made. Furthermore the second approach has the advantage that the original data can be stored and be available for engineering analysis, scientific processing and for developing new applications for these measurements. In addition, this second approach has the advantage of allowing a simpler environment to develop and debug the MDP processing (i.e. off-line, non real-time). For these reasons the second approach was implemented.

This decision shifted the difficult task from one of developing a real-time MDP algorithm to the implementation of high-speed transfer of large quantities of a data. This critical task was accomplished by streamlining the data transfer protocol between the DSP board and the main computer. At the end of each frequency step (actually each CIT, which may include more than one frequency step), the DSP memory contains a Doppler spectrum for each height/range, each of the four antennas and each of the two polarizations (also each frequency if several frequencies are multiplexed). This means that with each CIT up to 4096 Doppler spectra may be acquired in less than 2 seconds, even for a single frequency CIT (i.e. no frequency multiplexing). A Doppler spectrum typically contains 16, 32 or 64 Doppler bins where the amplitudes are represented by a logarithmically compressed complex two-byte quantity, for a total data volume on the order of

256 kilobytes. All of these data are transferred out of DSP memory, into off-line processing and/or written to a disk drive for storage.

1.2 Digital Receiver

Another important consideration was to replace the current analog receivers in the LP-DPS with new digital receivers. Major manufacturers like Harris Semiconductor and Analog Devices have announced new digital receiver IC's, but their availability is questionable at this time. On the other hand Graychip of Sunnyvale CA has for over three years been producing a quad digital receiver IC that is ideally suited to ionospheric sounding. The 60 MHz sampling rate is sufficient to cover the frequency range up to about 28 MHz, which is higher than most current analog sounders provide. Also, the four receivers per chip are fed by a single front-end analog-to-digital converter (ADC) making it possible to receive four frequencies simultaneously that can speed up sounding while using relatively long signal integration periods. For the Graychip 4014 the required RF bandwidth and integration of multiple receivers has not yet been achieved. Anticipating the availability of even more versatile digital receiver designs by other manufacturers as their technical capabilities improve, UMLCAR has begun the design of a digital receiver board that can be tested in a standard DPS ionosonde. Since all of the digital receiver IC's differ only in the details of the control interface logic, it is possible to design this interface into a programmable logic device (PLD) or field programmable gate array (FPGA). This approach minimizes the design changes necessary to insert a digital receiver from another manufacturer at a later date. We have chosen to use an FPGA since the entire interface can be realized in a single package, thus eliminating any possible unique wiring between logic devices.

1.3 Operational Test and Interference Analysis

The site in Puerto Rico (Ramey AFB) was chosen for the field trials because it represents a typical site that occasionally has problems with strong radio broadcast transmitters interfering with the reception of the sounder's pulse echoes. A test program was initiated and the initial results showed about the same level of interference with the operation of the Low Power DPS as with the DISS. These results have made it necessary to develop techniques that result in a significant reduction of these interference problems.

Shortly after installation of the new DPS sounder in Puerto Rico, it became apparent that HF interference and even echoes of the transmitted signals often overloaded the sounder

receiver. After analyzing the problem it was decided that this was mainly due to the more sensitive receiving loop antennas being used there. For the LP-DPS tests, the DISS receiving loops were used that are over 6 m across rather than the standard DPS 1.5 m diameter PVC loops. The received signal was therefore so much stronger than the system was designed to receive. In addition the antenna amplifiers used were set for a higher gain than the DISS preamplifiers. This combination made the receiver input signal much too large for the DPS receiver to handle, resulting in consistent bite-outs in the ionogram received signals whenever the receiver was at or near saturation. This happened particularly in the evening hours over the duration of these operational tests. A typical example of these bite-outs is shown in Figure 1 that is characteristic for the early evening and nighttime periods.

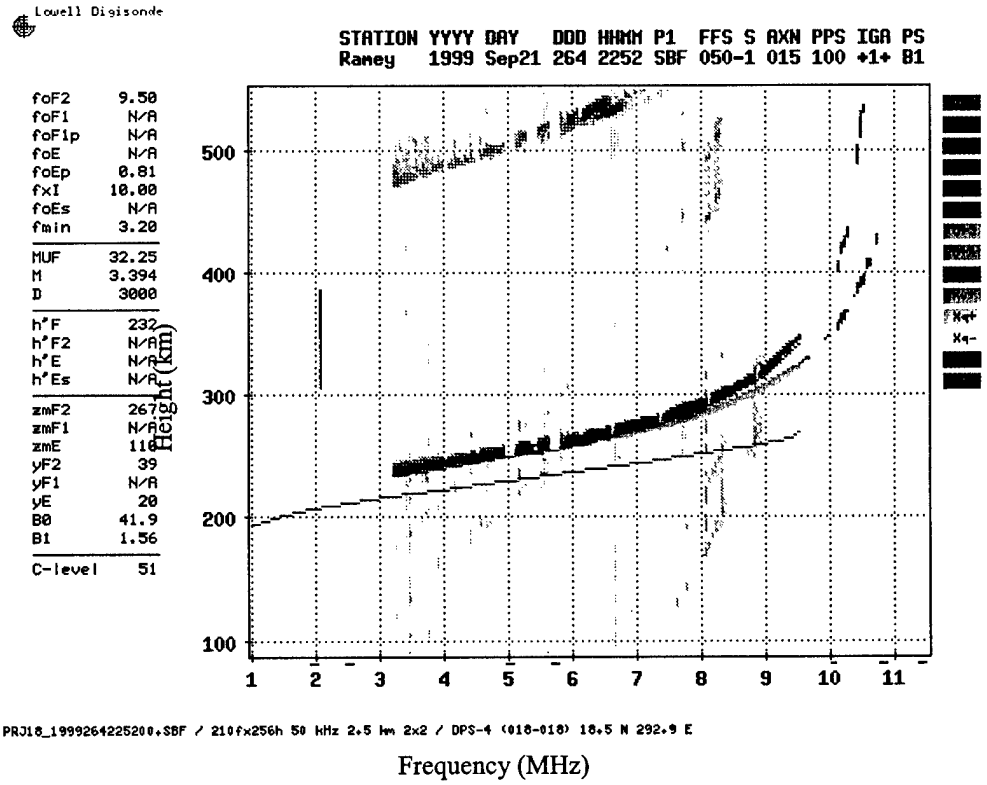

Figure 1. Sample Ramey ionogram showing frequency bite-outs between 9.5 and 10 MHz at 2252 UT caused by broadcast interference.

After sunset international broadcast stations usually become much stronger because D-layer signal absorption in the ionosphere decreases rapidly after that time. The first attempt to reduce the non-linear effects in the receiver front-end first was to change the sounder station

dependent gain setting, thereby reducing the first stage amplification in the receiver. Next, a program change was made to decrease the front-end gain. Finally, we modified the computer controlled automatic gain steps to allow more attenuation to be added when strong signals were detected. However, none of these steps modified the occurrence of the bite-outs particularly in the 9.5 to 10 MHz broadcast band.

Figure 2 shows another effect of these strong signals, that is making several multiple hop traces visible, at times up to seven, which often confused the ARTIST scaling program. The automatic gain adjustments normally keep the system from magnifying these weak signals, but these adjustments were already at the maximum attenuation in the original DPS configuration. The reduction of the overall receiver gain improved the automatic scaling to such a degree that after the change well over 90% of the ionograms were correctly scaled. Now even scaling difficult traces with bite-outs in them as shown in Figure 3 was accomplished.

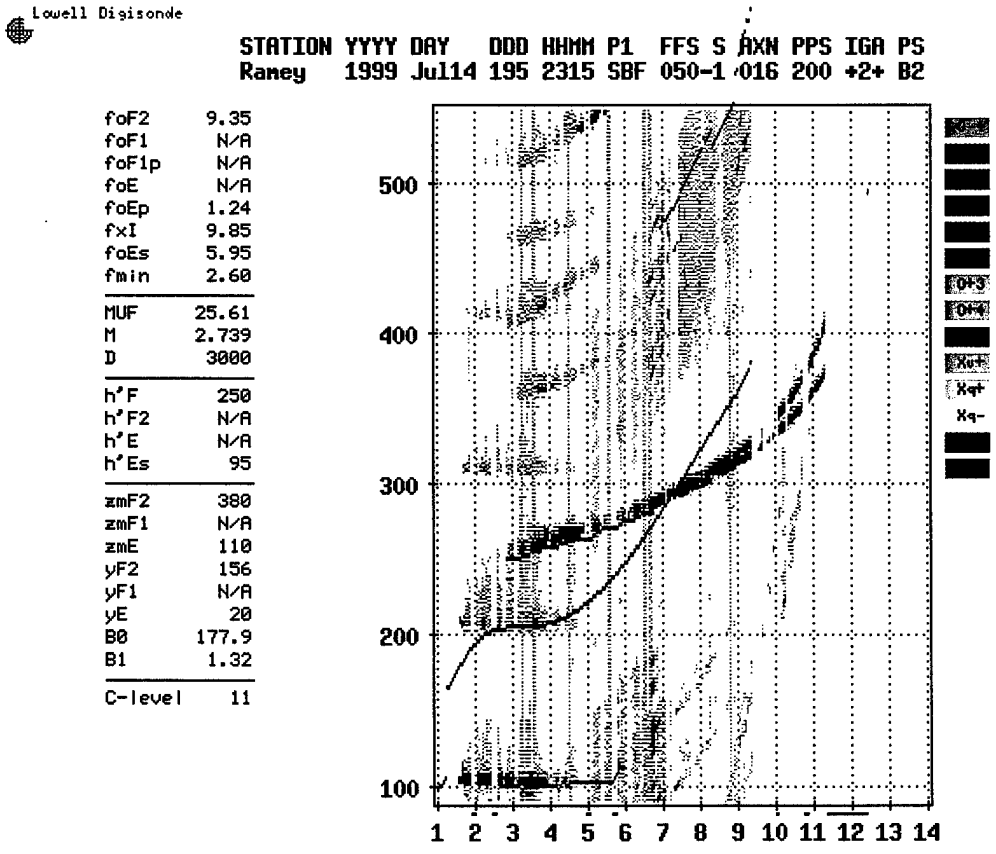

Figure 2. Excessive gain in the LP-DISS made weak signals strong enough to confuse the ARTIST scaling program.

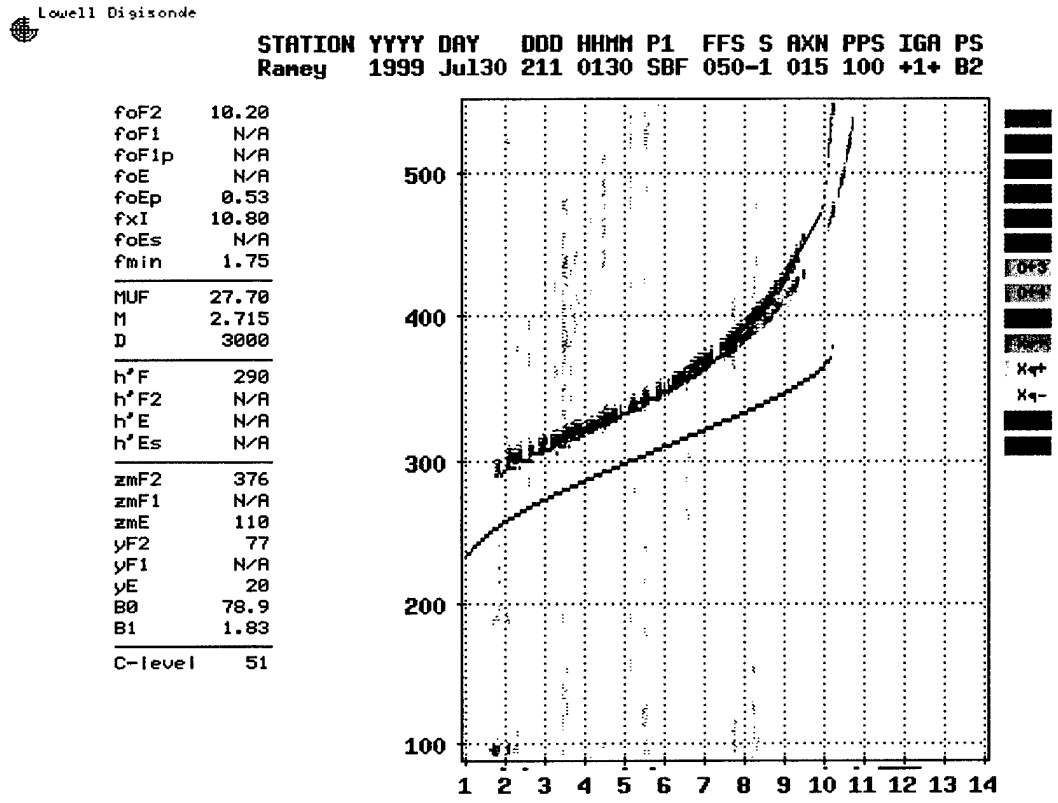

Figure 3. Correct ARTIST scaling across frequency bite-outs.

At Ramey, further improvement was achieved by replacing the antenna preamplifiers in the large loops with new ones that were set to have 12 dB lower gain. Also, the new preamplifiers optimized a critical amplifier interface (in the preamp circuitry), which provided an additional 6 dB margin against saturation. In spite of these considerable improvements to the Ramey system the occurrence of the bite-outs in the ionogram traces persisted. Measurements of the receiver front-end input signals indicated levels of 20 to 40 mV (including in-band interference). This led to the conclusion that the receiver is being saturated, not by non-linear effects converting an out-of-band signal into the receiver channel, but by in-band interferers operating on or near the sounding frequency. It then became necessary to investigate the characteristics of these interfering signals that make up these international broadcast bands.

The situation is not very different with the measurements from the older DISS system. The same bite-out effect is clearly seen in Figures 4 and 5. However, after reviewing many examples it became clear that the DGS256 succeeds on a significantly larger percentage of ionograms, using a few visible echoes to link the gap, giving the ARTIST scaling program the "stepping stones" it needed to link the short trace above 10MHz to the rest of the F-layer trace. Since the LP-DPS theoretically has enough signal processing gain to produce the same detection threshold as the older DISS, it was surprising that it failed more consistently. The major significant difference between the systems is that the DPS uses twice the signal bandwidth as compared to the DGS256, 30 kHz rather than 15 kHz.

If the international broadcast transmissions occur at randomly spaced frequencies, they will have some interval of clear bandwidth between them, with a mean free spacing roughly equal to the total unoccupied bandwidth divided by the number of transmitters present. Since the necessary spacing for the DPS to find a clear channel is 30 kHz (6 or more broadcast channels each with a bandwidth of 5 kHz), whereas the 15 kHz bandwidth of the DGS is only 3 channels wide. The probability of finding twice as many adjacent 5 kHz channels out of a large pool of random, uniformly distributed channels is proportional to the square of the required number. For our purposes this makes the DISS's clear-channel-search approximately four times more likely to succeed. Both ionosondes have a frequency search algorithm, which makes a quick scan of five candidate offsets around each nominal frequency step. The quietest frequency of the five is then chosen to make the measurement for that step in the ionogram.

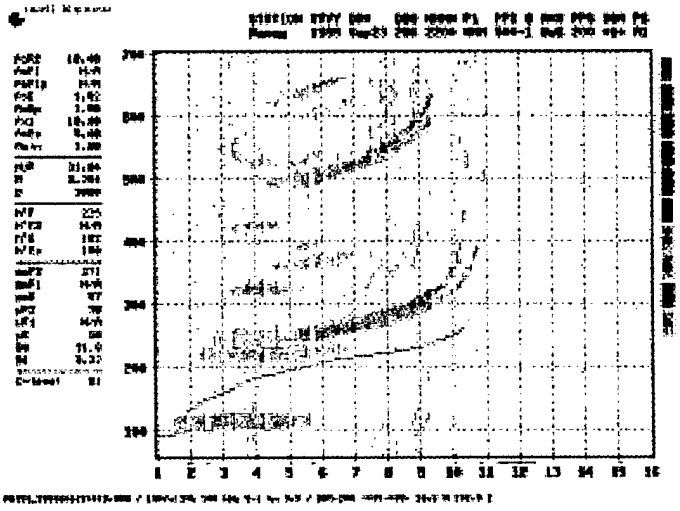

Figure 4. Ramey DISS ionogram at 2200 UT (early evening) on day 266.

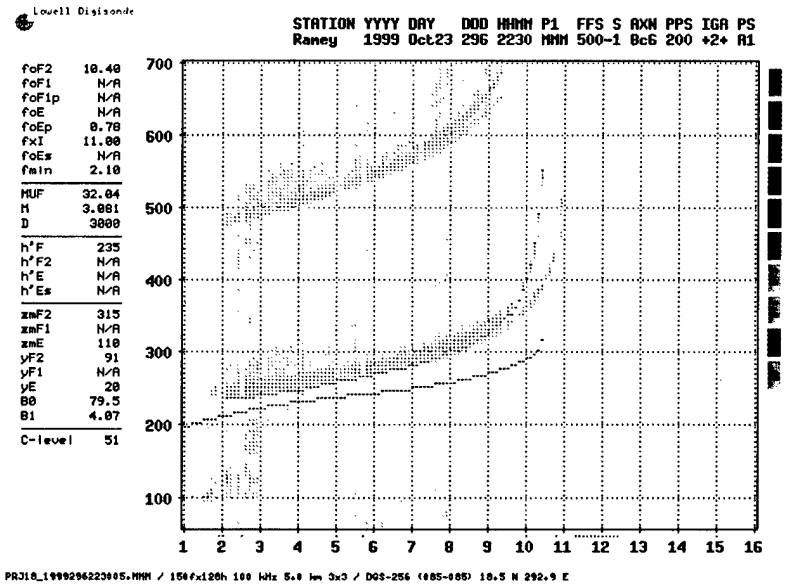

Figure 5. DISS ionogram at 2230 UT (early evening) on day 296.

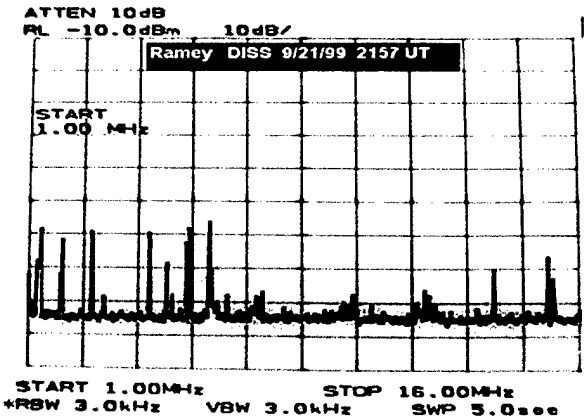

Figure 6. Daytime HF spectrum from 1 to 16 MHz. The DPS system is sensitive to echo signals 30 dB below the spectrum analyzed noise floor of –95 dBm.

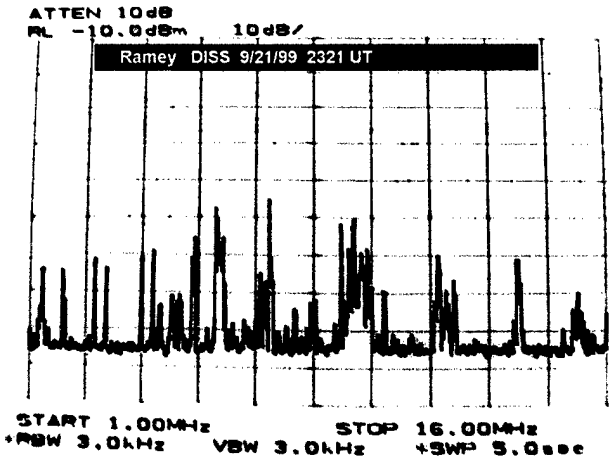

Figure 7. The nighttime HF Spectrum received on 1.5 m diameter loop. 10dB/vertical division and 1.5 MHz/horizontal division.

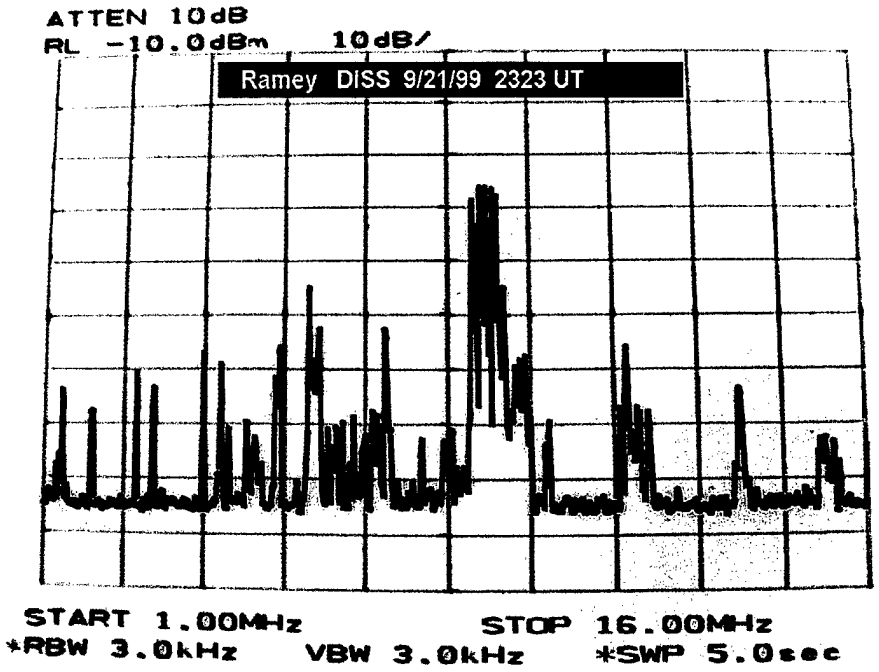

Figure 8. The nighttime HF Spectrum from 1-16 MHz as received on a DISS 6.5 m loop. 10dB/vertical division and 1.5 MHz/horizontal division.

Figures 6 and 7 show the amplitudes at the receiver impact during day and nighttime in the interference levels received with the 1.5 m small loop antennas. Only a small trace of the 6 MHz broadcast band appears above the –95dBm threshold of the spectrum analyzer, while the 7, 9, and 11 MHz bands are nearly invisible. In Figure 8 using the large DISS loop antenna, a strong enhancement at 9MHz is seen near the antenna's resonance. The small 1.5 m loop was not near resonance and a DPS antenna preamplifier was used, which loads down the higher frequencies to achieve a flatter response across the 1MHz to 40MHz operating range. The fact that both the large loop and small loop had about the same response showed that the DPS was not primarily degraded by large out-of-band signals in the receiver front end, but by in-band signals.

Two things work against the DPS with its 30 kHz bandwidth. First, the frequency search is not as effective because it only tests ±20 kHz around the nominal frequency. This is a total possible frequency change of 40 kHz, and with a 30 kHz bandwidth, clearly not very effective. Second, referring to Figure 9 it is clear that finding a clear 30 kHz channel will always be much more difficult.

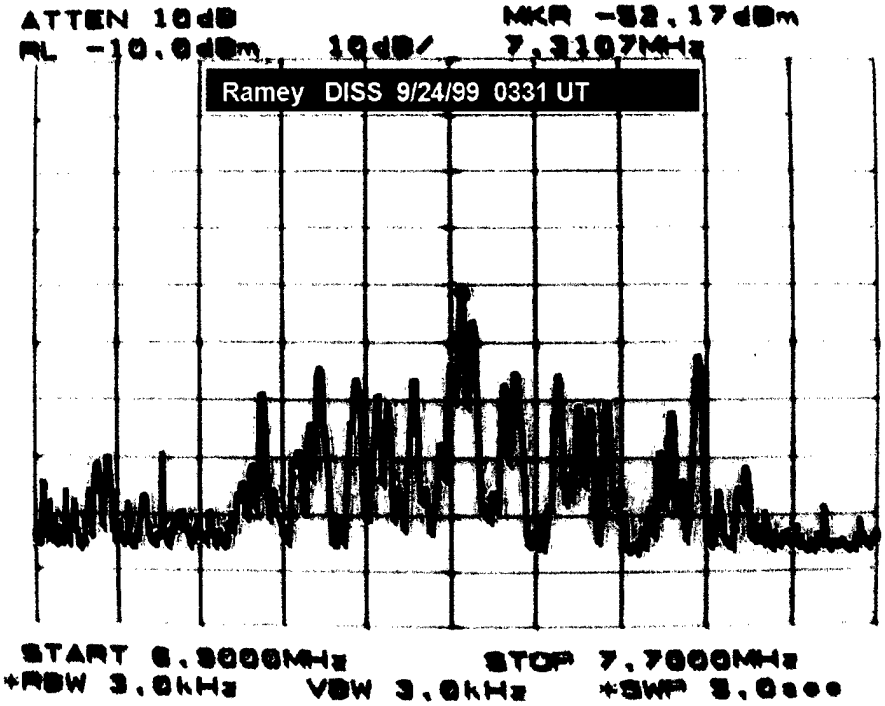

Figure 9. 7 MHz broadcast band from 6.9-7.7 MHz at 0331 UT (night). 10 dB/vertical division, 80 kHz/ horizontal division.

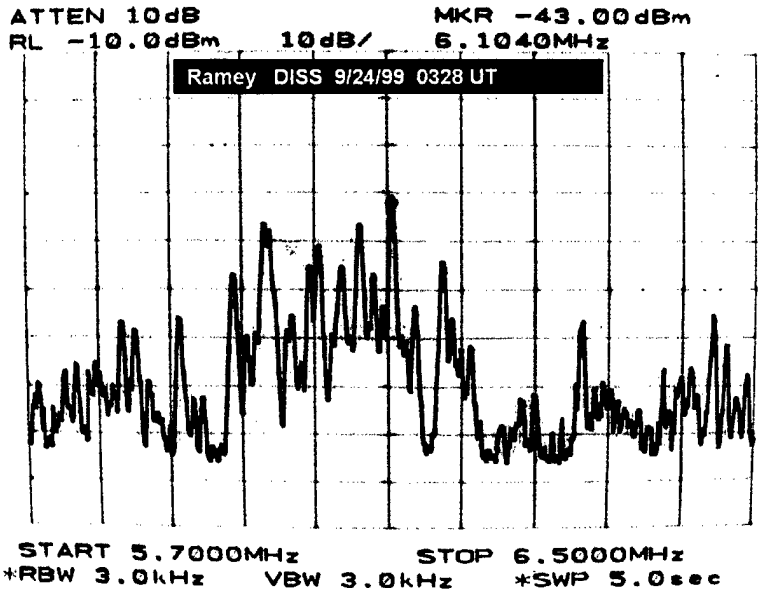

Figure 10. 6 MHz International Broadcast Band at 0328 UT. 10dB/vertical division, 80kHz/horizontal division.

One obvious conclusion is that the LP-DISS should be built with a 15 kHz bandwidth, using 8-chip Complementary codes rather than 16-chip. This is the original design of the DPS, before modifications were made to fulfill requirements in a recent commercial version. Another conclusion is that it would be very helpful to use one a techniques that eliminates these narrowband interfering signals early in the signal processing flow. Since their location in frequency is not known ahead of time the class of techniques required is Adaptive Interference Cancellation (AIC).

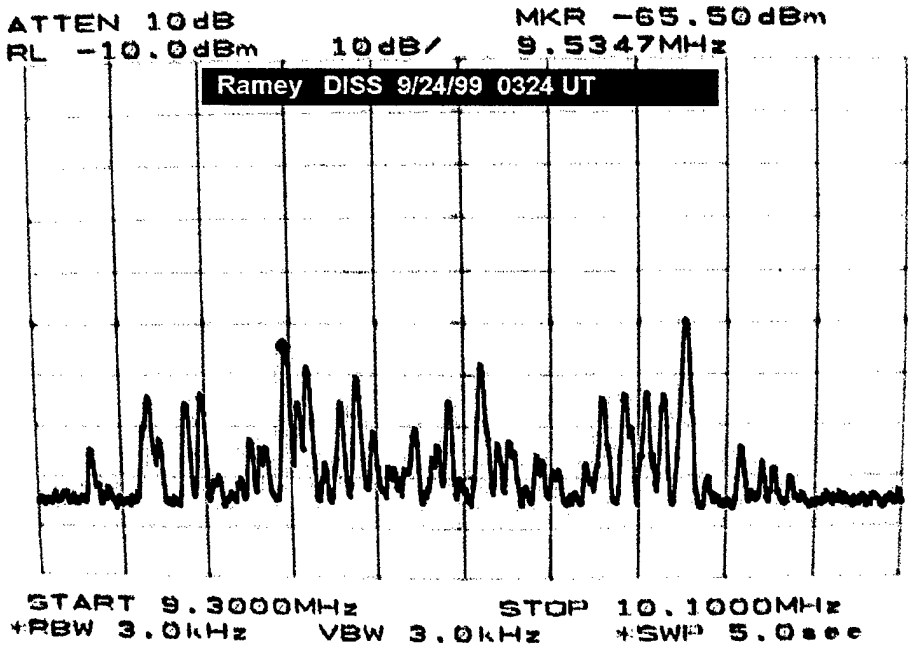

Figure 11. 9 MHz Radio Broadcast Band at 0324 UT.
10dB/vertical division and 80kHz/horizontal division

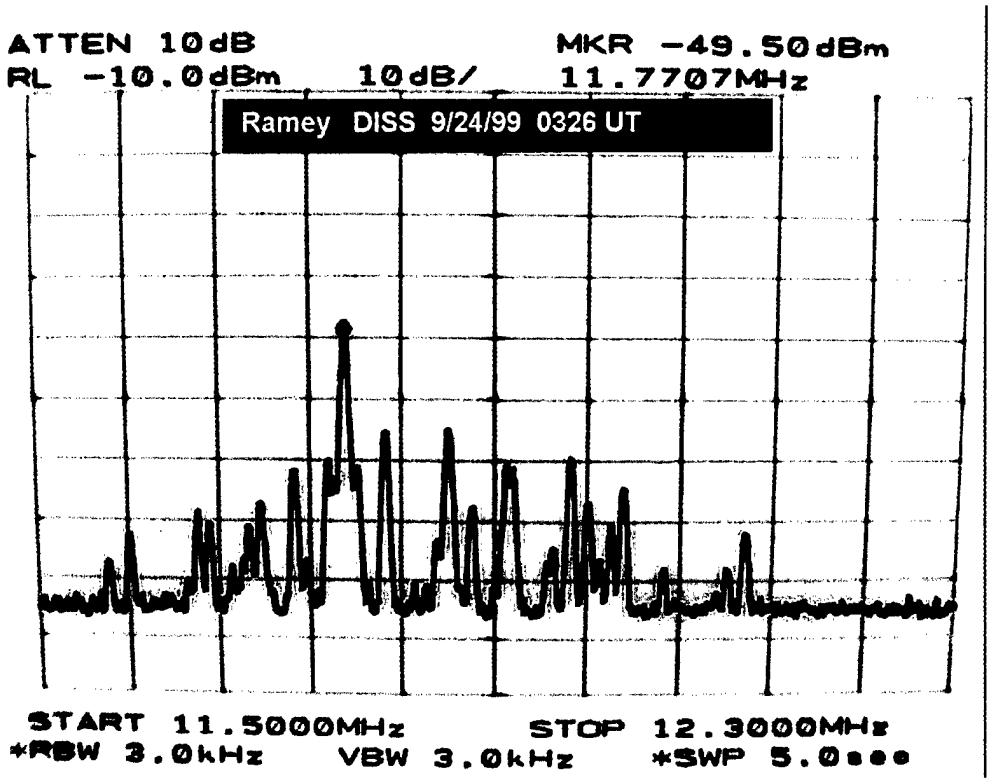

Figure 12. 11 MHz Radio Broadcast Band at 0326 UT.
10dB/vertical division and 80kHz/horizontal division.

1.4 Cancellation of Broadcast Transmitter signals double sideband AM modulation

There are three quite straightforward approaches to eliminating coherent (i.e. extremely narrowband) interfering signals in a broadband receiving system. They are:

1. Frequency Domain Excision – That is to delete strong spectral lines (more than a specified level above the mean amplitude) from the Fourier transformed signal in the spectral domain. This process is then followed by an inverse transform back to the time domain to restore the "cleaned" sample record.

2. Time Domain Excision – Here one estimates the amplitude and phase (using the transform of the sampled signal) of the interfering source and then subtracting it directly out of the sampled data record.

3. Adaptive Linear Prediction – Here one sets up a least-mean-square linear estimation loop to "predict" the next sample from the N previous samples. If the linear prediction loop is given a slow response time, it will predict the narrowband signal component but will not be able to "keep up with" the wideband signal.

These techniques work well for interfering signals that have energy confined primarily to one or to just a few spectral lines (the third approach especially can track changes out to several spectral line widths). The conclusion of this study is that the subtraction method (#2 above) is susceptible to changes in the modulation of the interfering signal, while the first method is degraded by spectral leakage that results from the Fourier property of assuming a periodic time domain function. Approach #2 has been successfully simulated. This approach seems feasible but with the limitation that it only succeeds in eliminating the narrowband component of the interfering signal and not the energy in the modulation sidebands. However, the carrier component is usually about 80% of the total signal power. Also, while the carrier aliases into the Digisonde range spectra as discrete lines, the modulation energy is more evenly distributed across the computed Doppler spectra.

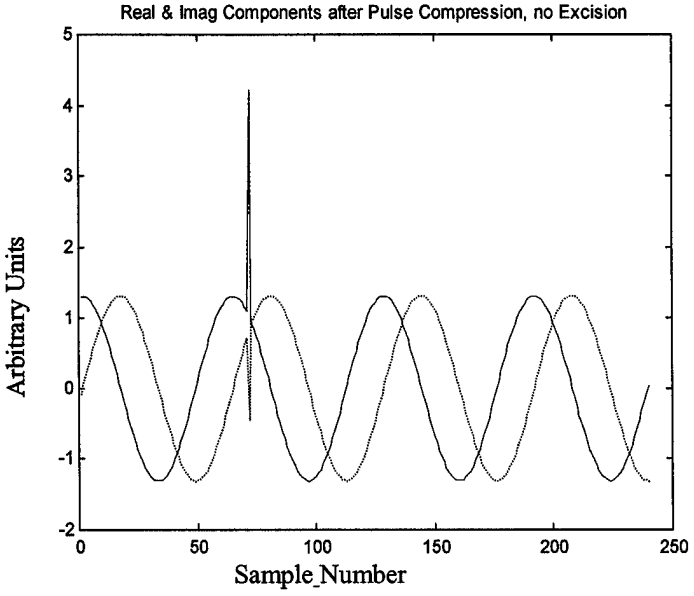

Figure 13. Pulse compressed signal received with one sinusoidal interferer 20 dB larger than the signal. Red (solid) is the real component and black (dotted) is the imaginary component.

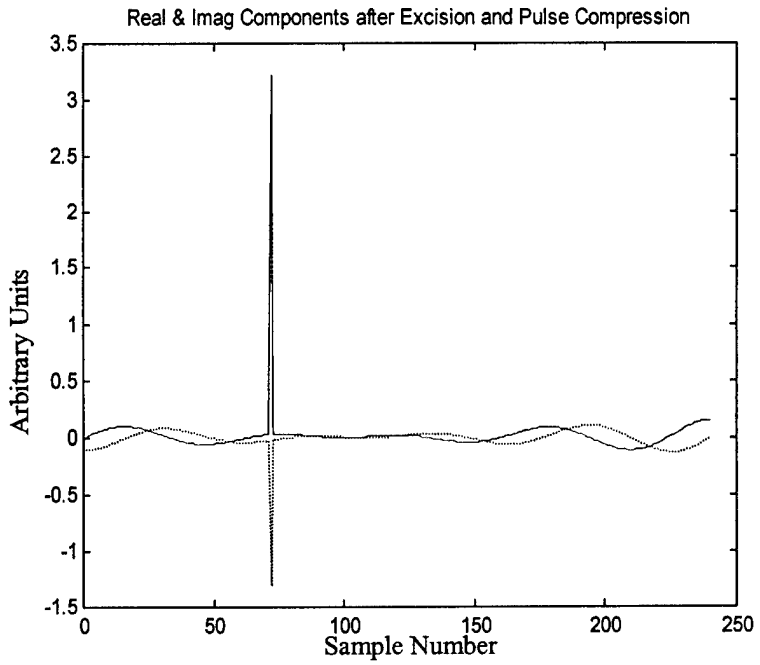

Figure 14. Pulse compressed signal of Figure 4 with +20 dB interferer removed by sine wave subtraction._Red (solid) is the real component and black (dotted) is the imaginary component.

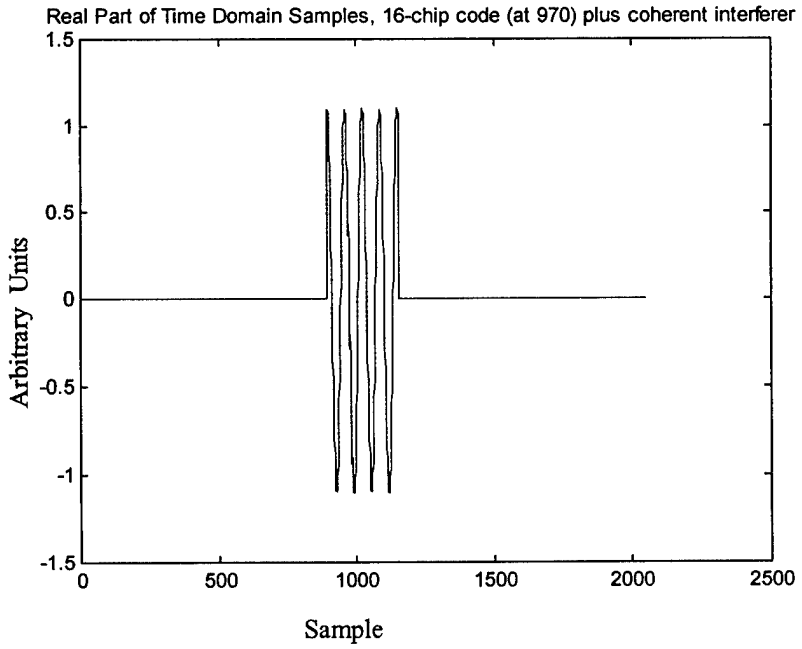

Figure 15. Raw signal samples (256 points) placed into larger array (2048 points) filled with zeros.

Figure 13 shows that with a -20 dB received signal-to-noise ratio, the DPS pulse compression alone is sufficient to allow echo detection. Figure 14 shows the improvement possible by subtracting a sine wave function (corresponding to the narrow band interferer) as detected in the spectral analysis of the sampled signal. The correct amplitude and phase of the interfering signal must be estimated quite accurately for this technique to be effective. An efficient algorithm using an artificially large (i.e. zero filled) sample array to make a large, high-resolution spectral array is explained as follows.

In Figures 13-19, the vertical axis is linear amplitude and the horizontal axis is sample number, which corresponds to linear steps in either time or frequency. Applied to the DPS, the time sample interval is 16.7 μs.

A sample record, consisting of 256 complex samples was placed in the middle of a buffer of 2048 complex elements as shown in Figure 15, with the rest of the array filled with zeroes. Note the small ripples just before sample 1000. This is the received phase-coded DPS pulse. The FFT transformation of this artificially large record provides 8 times more spectral resolution than if zeroes did not extend the time domain record. There is no increase in wanted signal resolution

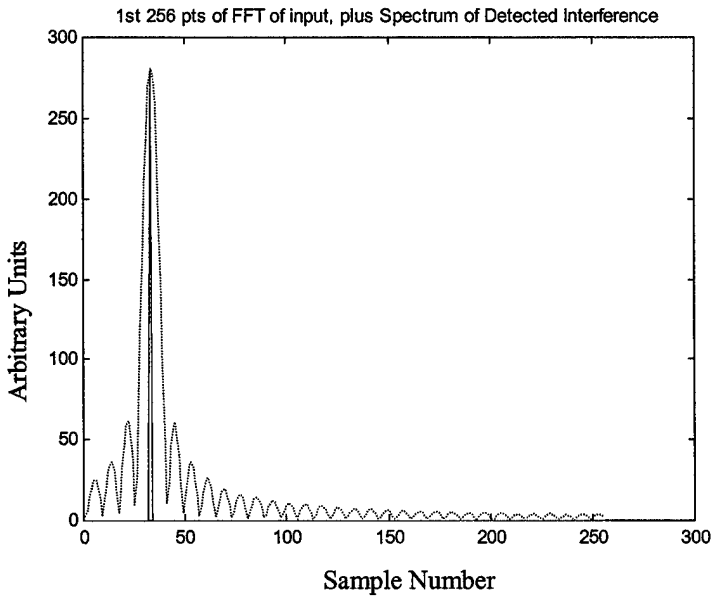

Figure 16. The two spectral lines selected to represent the interferer are shown with the surrounding 254 lines in the lowest one-eighth of the large transformed (spectral domain) array. The sidelobes are a result of the rectangular windowing of the time domain samples (the interferer is assumed to be unmodulated in this case). The red (solid) is the original interferer spectral lines and the black (dotted) is the processed interferer using the rectangular window.

so the higher resolution spectral lines better describe the shape of the central lobe of the transformed spectral line, and the leakage across the spectrum. The lower resolution FFT would only have a single spectral line for each lobe. This technique allows much finer detection of the actual frequency of the interferer, and the phase of the spectral line is also the correct time domain phase. If the frequency is determined with eight times the resolution (defined by the reciprocal of the sample period) then the reconstructed sine wave will be less than 45 degrees away from the actual interferer's phase. In fact, the phase is most correct at the center of the time domain record, therefore the maximum error at the ends is 22.5 degrees. Taking the two central lines at the peak of the spectral lobe as shown in Figure 16, and then taking the inverse transform in a zero-filled frequency domain array, provides a time domain function that covers the entire 2048 sample points, but is only correct in phase and amplitude over the interval of the original samples in the middle of the array. Therefore, by subtracting this function from the original samples, a "cleaned up" time domain function was achieved. This process is illustrated in Figure 17, where the continuous line big signal is the sum of the received signal consisting of a strong interferer and the 16-chip phase coded echo pulse. The dashed line is the inverse transform of the function shown in Figure 17 and the small-signal continuous line is the "cleaned up" difference.

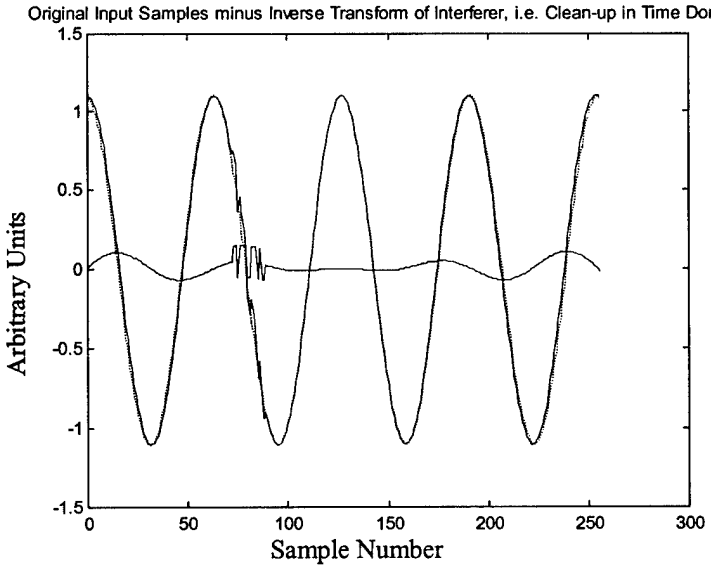

Figure 17. Time domain clean-up operation using amplitude and phase of the interferer estimated from the frequency domain analysis. The red (solid) is the original input samples and black (dotted) is the inverse transform of the interferer. The blue (solid) is the recovered signal.

At this point the large array can be reduced in size during the subtraction operation by shifting the array position of the computed difference term, *csig(n)*,

Re(csig(n)) = Re(lsig(n+384)) - Re(exc(n+384)

Im(csig(n)) = Im(lsig(n+384)) - Im(exc(n+384),

where *lsig* is the large zero-filled array containing the original signal samples and *exc* is the array containing the sinusoid to be subtracted from the original signal.

Figures 18 and 19 show similar results, using a Hamming window to taper the original sample array before the initial frequency transform. Now, four lines in the frequency domain were selected, which because of the windowing represent about 98% of the interference power, rather than 90% with the rectangular window and only two lines. The inverse transform generates a time domain signal with two more degrees of freedom, and therefore matches the time domain function slightly better. The result is to bring down the large interferer amplitude at the beginning of the time domain record. Using the Hamming window also reduces the effect of other interference signals that induce errors in our estimate of the phase and amplitude of any one interfering signal, that is, there is less leakage from one spectral line to another.

This is a very basic simulation where the real world would have multiple interferers of different phases and amplitudes. However, the more challenging issue in the "real world" is that these interfering signals are not constant amplitude spectral signals , although they have constant phase and frequency. The next section describes the effectiveness of this subtraction algorithm on modulated signals.

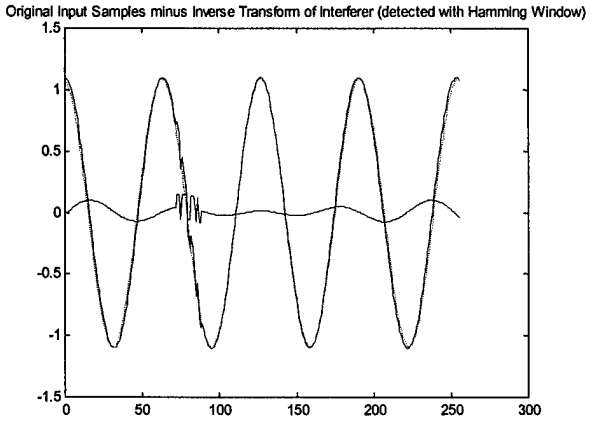

Figure 18. Same result as Figure 17 but first transform into the frequency domain used a Hamming window. The red (solid) is the original input samples and black (dotted) is the inverse transform of the interferer. The blue (solid) is the recovered signal.

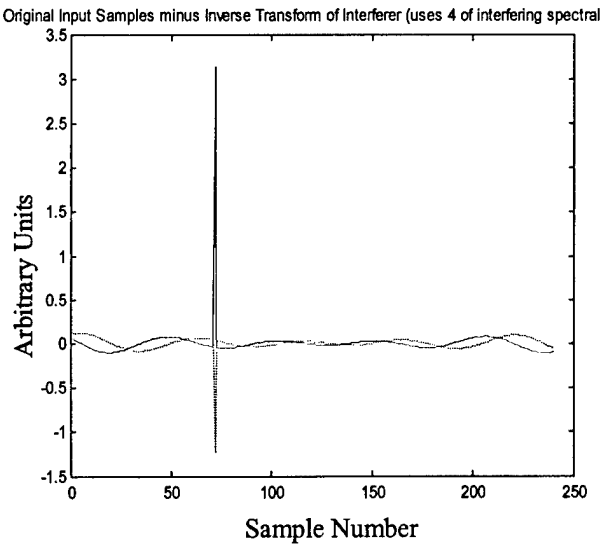

Figure 19. The cleaned up time domain signal derived from the Hamming weighted spectrum after pulse compression. Red (solid) is the real component and black (dotted) is the imaginary component.

Now consider the analysis of modulated interfering signals. The interferer signal from a broadcast transmitter has about a 1 Hz spectral width. This narrow bandwidth can only be realized if approximately one seconds worth of signal is integrated. In reality, echo signal sample records are only 8.5 ms long, and during this time, a significant change in the amplitude of the interfering signal may occur because of the AM modulation. . However, with AM double sideband modulation the frequency and the phase do not change. Given that the transmissions contain less than 3 kHz of modulation bandwidth we cannot expect the signal amplitude to vary in a time less than 150 μs. During the integration period the modulation can go through many cycles. Each time it goes through an amplitude cycle time the instantaneous frequency of the modulation signal can change. If the frequency of the modulation signal were to change 3 kHz in 150 μs that would constitute an FM modulation rate of 3 kHz and an FM modulation index of 1.0. A faster FM rate puts the modulation energy outside the 3 kHz signal bandwidth and that would be filtered out before the modulator, and therefore cannot exist in the received signal spectrum. A worst case is that the interfering signal as seen in a DPS receiver output can go through approximately 50 amplitude cycles. Since the frequency and phase cannot change, a very good approximation to the interfering frequency (using the eight times resolution technique

to accurately find the spectral peak) can be made. It is then possible to subtract a sinusoid that has the mean amplitude of the interfering signal over our sample period and a very close approximation to the carrier component of the signal can be achieved. .

The example of Figures 20 and 21 show the limit of the subtraction technique. The parameters are:

- Interferer frequency 470 Hz away from DPS operating frequency
- AM Modulation frequency is 187 Hz
- FM rate of information signal is 18 Hz/sec

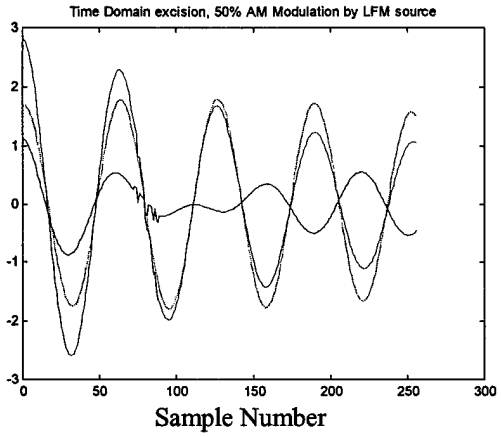

Figure 20. Time domain clean-up operation using amplitude and phase of the interferer estimated from the frequency domain analysis. The red (solid) is the original input samples and black (dotted) is the inverse transform of the interferer. The blue (solid) is the recovered signal.

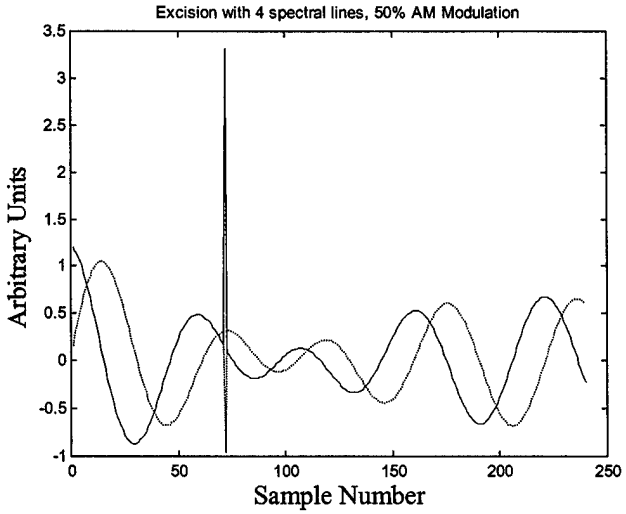

Figure 21. Sinusoid subtraction of a fixed amplitude sinusoid from an AM modulated signal after pulse compression. Red (solid) is the real component and black (dotted) is the imaginary component.

Note that in Figure 20 the amplitude of the modulating signal is monotonically decreasing, and the dashed line, which is the sinusoid to be subtracted (constant amplitude) is a "best approximation" to the interfering signal, making it a replica of the carrier component of the interfering signal. The simplicity of this example is contrasted to a "worst case" in the next example. The conclusion is that in both cases only the carrier component of the signal is being cancelled. Therefore, it doesn't make any difference as to the spectral content of the modulation. Only the carrier energy, which is the most significant contributor, is eliminated.

Now a more challenging case is considered. During the 8.5 ms sample time the interferer is being modulated 50% by a 1 kHz tone, which sweeps linearly up to 2 kHz by the end of the sample record. The carrier itself is constant in frequency and phase, only the modulating envelope is changing (SNR is still -20 dB). The spectrum in Figure 22 shows the modulation sidelobes. In the extreme right of the spectrum of Figure 22 one can see the faster periodicity of the sidelobes as expected from the sinc function of an unmodulated interferer. Figure 23 illustrates the steps in the process, the original samples, the estimate of the interferer, and the cleaned-up signal after the subtraction operation has been performed. Figure 24 shows the final compressed pulse with no interferer excision, the "before" case, while Figure 25 shows the "after", or "cleaned" case.

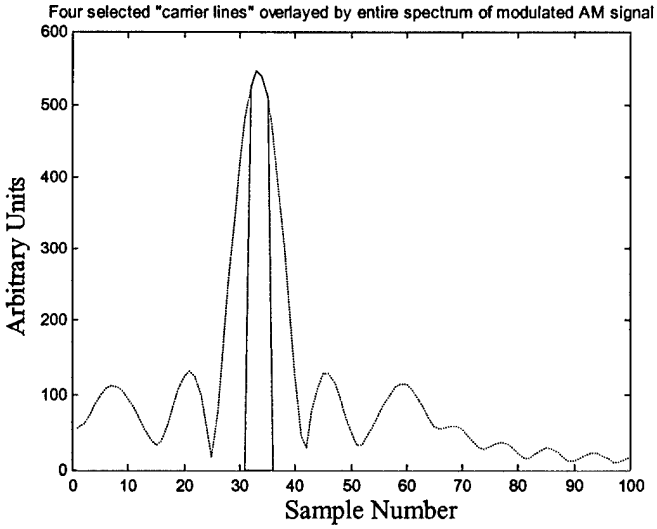

Figure 22. Dotted line (black) shows spectrum of LFM/AM modulated interferer. Solid line (red) shows detection of interferer.

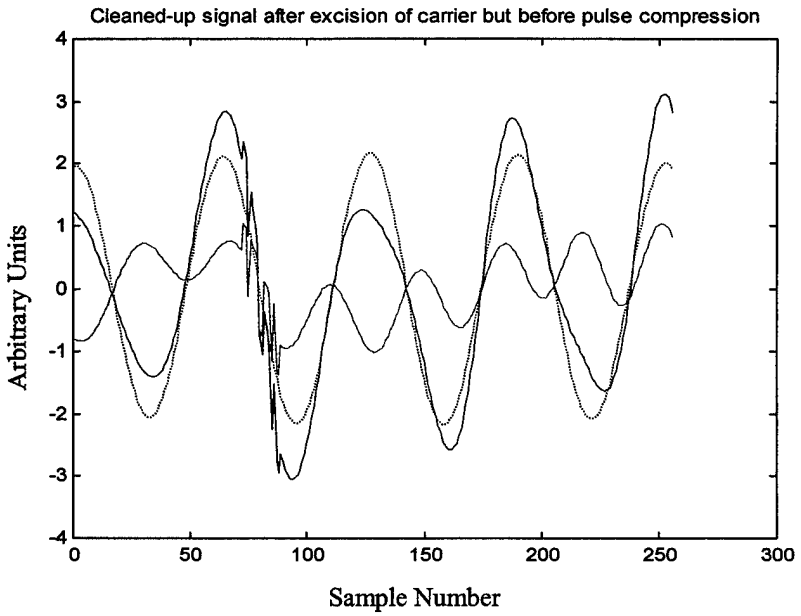

Figure 23. Signal and interferer before pulse compression. The three lines show the contaminated original sample (red/solid), the interferer signal to be excised (black/dotted), and the cleaned-up signal (green).

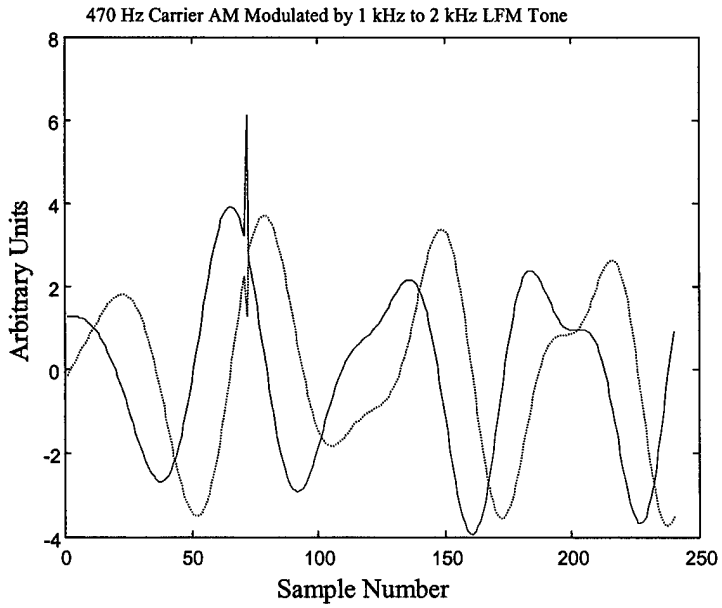

Figure 24. Signal with amplitude modulated interferer after pulse compression (no excision). Red (solid) is the real component and black (dotted) is the imaginary component.

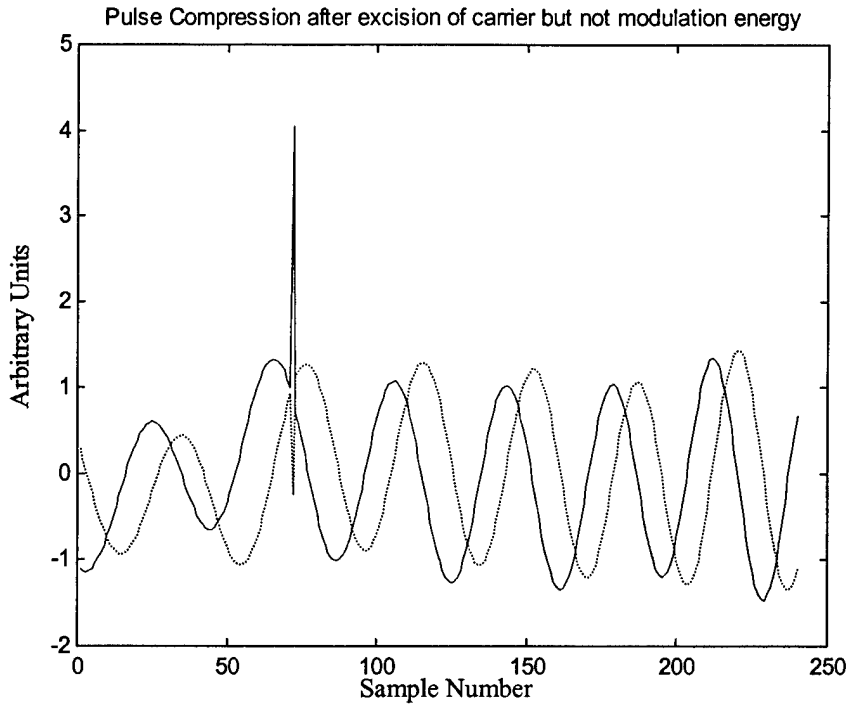

Figure 25. Signal after pulse compression (no Doppler integration) with interferer excision. Red (solid) is the real component and black (dotted) is the imaginary component.

2.0 Conclusions

These new interferer suppression techniques can be implemented and tested at an actual sounding site (e.g. Ramey AFB, Puerto Rico) with the potential to produce a better sounding system that is less affected by the inteferers within the international broadcast bands, particularly after sunset. The resulting echo traces will be more easily analyzed by the ARTIST software, yielding a higher percentage of correctly scaled ionograms. A new technique of determining the precise frequency of strong inteferers and the amplitude and phase has been suggested by K. Bibl. Subtracting this signal from the received signal in the time domain, and successively applying this process to several interferers would significantly enhance the LP-DISS performance.